Contents lists available at ScienceDirect

South African Journal of Chemical Engineering

journal homepage: http://www.journals.elsevier.com/south-african-journal-of-chemical-engineering

Prediction of hydrodynamic characteristics of a venturi scrubber by using CFD simulation

Manisha Bal [a], *Bhim Charan Meikap* [a,b,*]

[a] *Indian Institute of Technology (IIT) Kharagpur, Department of Chemical Engineering, West Bengal 721302, India*
[b] *School of Engineering, Howard College, King George V Avenue, University of Kwazulu-Natal, Department of Chemical Engineering, Durban 4000, South Africa*

ARTICLE INFO

Article history:
Received 17 August 2017
Received in revised form
4 October 2017
Accepted 24 October 2017

Keywords:
Venturi scrubber
Hydrodynamics
Pressure drop
Computational fluid dynamics
Nuclear power plant safety
Flow prediction

ABSTRACT

The filtered containment venting system (FCVS) is a safety relevant system, which consists of venturi scrubber and a mesh filter. FCVS needs to be further assessed to improve the existing performance of the venturi scrubber. Therefore, hydrodynamics is an important counter-component needs to be investigated to improve the design of the venturi scrubber. In the present research, Computational Fluid Dynamic (CFD) has been used to predict the hydrodynamic behaviour of a newly designed venturi scrubber. Mesh was developed by gambit 2.4.6 and ansys fluent 15 has been used to predict the pressure drop profile inside the venturi scrubber under various flow conditions. The Reynolds Renormalization Group (RNG) k-ε turbulence model and the volume of the fluid (VOF) were employed for this simulation. The effect of throat gas velocity, liquid mass flow rate, and liquid loading on pressure drop was studied. Maximum pressure drop 2064.34 pa was achieved at the throat gas velocity of 60 m/s and liquid flow rate of 0.033 kg/s and minimum pressure drop 373.51 pa was achieved at the throat gas velocity of 24 m/s and liquid flow rate of 0.016 kg/s. The results of the present study will assist for proper functioning of venturi scrubber.

1. Introduction

Venturi scrubber is well-known device for controlling the particulate matter and gaseous emission in industry (Desai and Sahu, 2014). Recently it is gained importance for the removal of radioactive material in filtered containment venting system in nuclear power plant. Fukushima daichii accident has reinforced the necessity to further improve safety in nuclear power plant design (Shozugawa et al., 2012). So, filtered containment venting system is now necessary to install in nuclear power plant to protect the integrity of containment and to collect the aerosol and iodine particle from the radioactive exhaust gas (Rust et al., 1995). Venturi scrubber successfully removes the fine particle for its design. It is basically consists of the three sections: convergent section, throat section and divergent section. Throat section of venturi scrubber pushes the gas stream to accelerate as the duct narrows and then expands, causes increase in gas velocity and turbulence. Scrubbing liquid injected either at the throat section or convergent section,

* Corresponding author. Department of Chemical Engineering, School of Engineering, Howard College, University of KwaZulu-Natal, Durban, South Africa.
E-mail address: bcmeikap@che.iitkgp.ernet.in (B.C. Meikap).
https://doi.org/10.1016/j.sajce.2017.10.006

produces the tiny droplets by contacting with high gas velocity. Particulate matters are captured by these droplets. In the diffuser section, deaceleration of the gas section occurs by recovering the pressure (Gamisans et al., 2002; Swamy et al., 2015). Computational fluid dynamics has an enormous potential impact on industry because the solution of the equation of motion provided everything that is meaningful to know about the domain. Ansys fluent is one of the most powerful tool of CFD software, provides the modelling of fluid and other physical phenomenon (Sripriya et al., 2007; Goniva et al., 2009; Bayatian et al., 2016). The main objective of this paper is to design an efficient filtered containment venting system which can be used in the nuclear power plant. A venturi scrubber has been designed here. Before the performance study, knowledge about hydrodynamic study inside venturi scrubber is very important. Pressure drop is the very significant parameter for the venturi scrubber. It quantifies the power consumption which estimates the efficiency of the scrubber (Biswas et al., 2008). In the present research, fluid flow behaviour in venturi scrubber has been studied using ansys fluent. The effect of different parameters on the pressure drop of venturi scrubber is also investigated for the smooth operation.

2. Literature review

Performance of venturi scrubber depends on the pressure drop generated at the throat section. Wall frictional loss and acceleration loss are mainly causes the pressure drop in venturi scrubber. Many mathematical model and computational model have been developed to evaluate the pressure drop in venturi scrubber such as that proposed by Calvert (1970), Boll (1973), and Leith et al. (1985). Recently many computational models are also developed to predict the flow behaviour in venturi scrubber. In a rectangular, pilot scale Pease Anthony type venturi scrubber, effect of nozzle arrangement on flux distribution was studied by Ananthanarayanan and Viswanathan (1999) using CFD package fluent. Four nozzles configuration were taken to study the flux patterns which determined the non-uniformity flux distribution rises when nozzle to nozzle distance reached 10% of the side width where nozzle was placed. It was found that the nozzle diameter or liquid rate had great effect on multiple jet penetration which gave 10–45% less liquid than uniform penetration. Pak and Chang (2006) studied the collection efficiency by the computational model for gas-dust-liquid flow in venturi scrubber. Eulerian-Lagrangian approach was adopted to solve the numerical model. Numerical results were validated with previous experimental data. Goniva et al. (2009) used open foam framework in his research to determine the capturing efficiency. Eulerian–Lagrangian approach was adopted to estimate the efficiency. Dust particles were captured by the impaction, diffusion and interception. Coalescence model and break up model measured the size distribution of Liquid droplet. Ahmadvand and Talaie (2010) followed Eulerian approach to simulate the two dimensional mathematical model of droplet dispersion. K-ε turbulence model was applied to estimate gas field and eddy diffusivity along the venturi scrubber. Droplet concentration distribution was predicted by mass balance of droplets and eddy diffusivity of droplets was calculated by the Fathikalajahi and Talaie (1997) method. Rosin-Rammler distribution had been taken into account for droplet size distribution. Results gave good agreement with experiment result at constant peclet number. Ali et al. (2012) evaluated the pressure drop by the computational fluid dynamics. They had used ANSYS CFX tool in which k-ε turbulence model was employed to find the hydrodynamics of scrubber. Later Ali et al. (2013) presented the dust removal efficiency using CFD simulation in ANSYS CFX. Eulerian-Lagrangian approach was used to find the efficiency. Break up model of liquid followed the cascade atomization and break up model. Gulhane et al. (2015) used the ANSYS Workbench tool to predict the pressure drop in their research work. Eulerian–Eulerian approach was followed to understand the hydrodynamic behaviour.

3. Venturi scrubber geometry

Dimension of venturi scrubber is shown in Fig. 1. Mesh of 3D circular venturi scrubber was created in gambit 2.4.6 (ANSYS Fluent Meshing User's Guide, 2015). Ansys fluent 15 is applied to do the solution (ANSYS: Fluent User's Guide, 2015). Steady state condition has been adopted. Renormalization (RNG) K- ε turbulent model and VOF are used to simulate the gas flow. RNG model is very favourable for separated flows and recirculation flows such as sudden expansions, forward or backward facing steps that may occur in venturi scrubber and also have greater reliability and representativeness. VOF model is applied to track the liquid gas interfaces, and it could be used to a steady state simulation. Closed wall surfaces treated as standard wall function. In this work, hybrid mesh had 151923 cells, with 312381 faces and 29760 nodes. Grid independency test is also done to ensure the solution was independent on the mesh density. Three mesh densities are chosen for the optimization of mesh, which contained 202461, 151923,108718 mesh densities. Pressure drop at liquid to gas ratio 0.6×10^{-3} $m^3/m^3$and liquid mass flow rate 0.016 kg/s is similar for 202461 and 151923 mesh densities. Therefore, 151923 mesh density is selected for entire simulation. The boundary conditions adopted to do the solution are as follows: Air entry at the top of the convergent section is prescribed as mass flow rate inlet and exit of air and liquid is taken as atmospheric pressure; Liquid injection is prescribed mass flow rate at the face; non-slip condition at the wall. CFD ANSYS FLUENT 15.0 is chosen to solve this numerical problem through the VOF method and it is applied to the solution of the incompressible and isothermal two-phase flow. SIMPLE algorithm is used to solve the pressure-velocity coupling. 1st order upwind scheme is selected for momentum equation and turbulent dissipation rate is solved by First order upwind scheme. 10^{-4} is selected as the convergence criteria for all problem variables and relaxation parameters have been chosen in the range of 0.3–1.

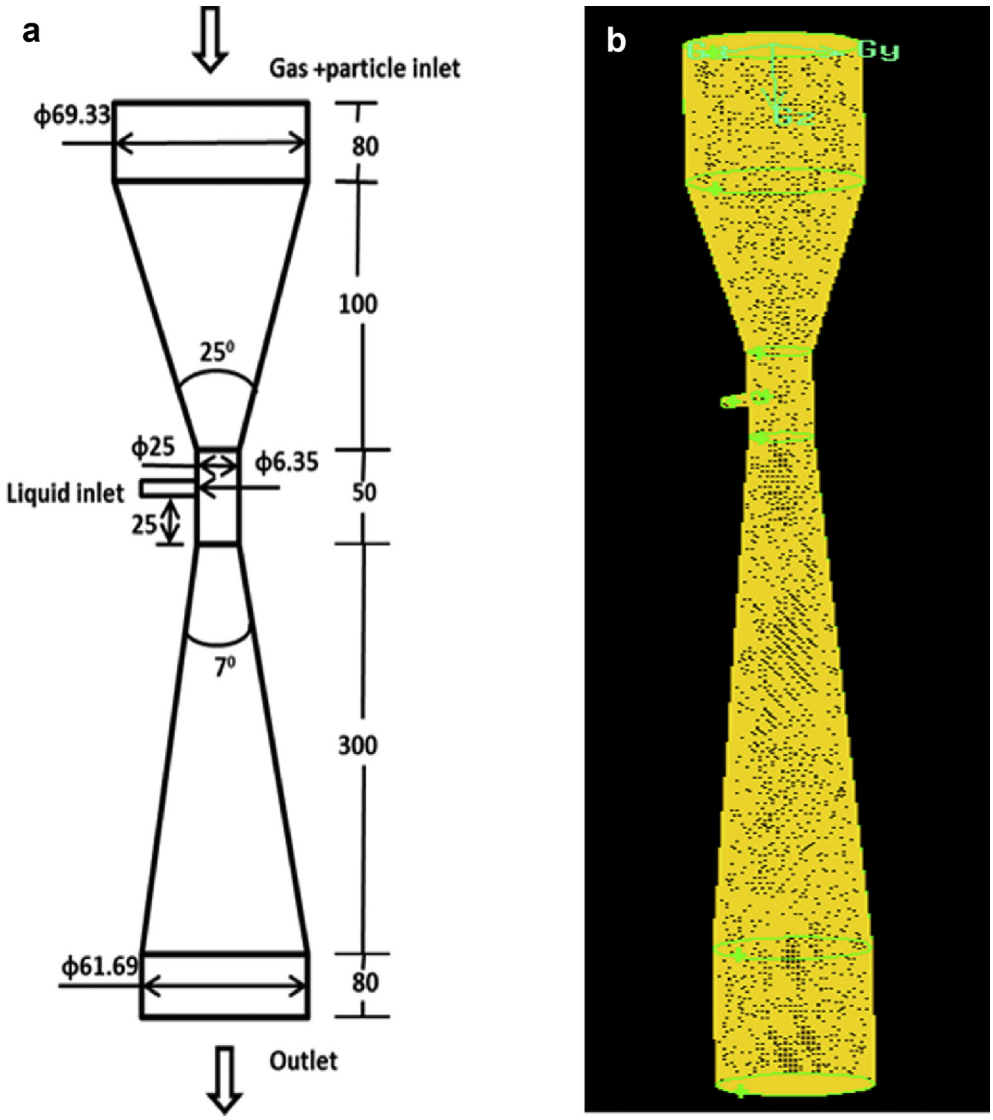

Fig. 1 – a: Geometry of venturi scrubber (in mm). b: Mesh of the geometry.

4. Numerical model

4.1. *Transport equations for the RNG k-ε model*

Gas flow field is solved by the Eulerian approach using RNG k-ε turbulence model by considering standard wall function (Guerra et al., 2012; Bayatian et al., 2016). The instantaneous Navier-Stokes equations is used to obtain the RNG k- ε turbulence model, which is solved by a mathematical technique called "Renormalization group" (RNG) methods. Transport equations for the turbulent kinetic energy (k) and turbulent dissipation (ε) are shown in the Eqs. (1) and (2) respectively.

Transport equation for turbulent kinetic energy (k)-

$$\frac{\partial(\rho k)}{\partial t}+\frac{\partial(\rho k u_i)}{\partial x_i}=\frac{\partial}{\partial x_j}\left(\alpha_k\mu_t\frac{\partial k}{\partial x_j}\right)+G_k+G_b-\rho\varepsilon-Y_m+S_k \quad (1)$$

Transport equation for turbulent dissipation (ε)-

$$\frac{\partial(\rho\varepsilon)}{\partial t}+\frac{\partial(\rho\varepsilon u_i)}{\partial x_i}=\frac{\partial}{\partial x_j}\left(\alpha_\varepsilon\mu_t\frac{\partial\varepsilon}{\partial x_j}\right)+c_{1\varepsilon}\frac{\varepsilon}{k}(G_k+C_{3\varepsilon}G_b)-C_{2\varepsilon}\rho\frac{\varepsilon^2}{k}-R_\varepsilon+S_\varepsilon \quad (2)$$

In these equations, S_k and S_ε are source terms that defines the interaction with droplets.

4.2. *VOF model*

VOF model is implemented for its better performance in phase interaction than the lagrangian approach (Guerra et al., 2012; ANSYS: Fluent User's Guide, 2015). In the present work, isothermal, turbulent, incompressible two phase flows are considered. Conservation of momentum follows the Eq. (3) which shown below.

Momentum equation

$$\frac{\partial}{\partial t}(\rho\bar{v})+\Delta\cdot(\rho\bar{v}\bar{v})=-\Delta p+\Delta\cdot\left[\mu\left(\nabla\bar{v}+\nabla\bar{v}^T\right)\right]+\rho\bar{g}+\bar{\bar{F}} \quad (3)$$

In Eq. (3), ρ and μ are the density and viscosity of the mixture and they are dependent on the volume fraction of each phase in a computational cell. $\bar{v}$ represents the velocity vector.

Transport equation of the volumetric fraction

$$\frac{d\alpha_q}{dt}+u\Delta\alpha_q=0 \quad (4)$$

5. Results and discussion

Contaminated gas fed into the venturi scrubber at the top portion of the convergent section at a certain gas flow rate, and scrubbing liquid is injected at the throat section. Maximum gas velocity is obtained at the throat gas section due to small cross sectional area. Gas with high kinetic energy hits the liquid to produce tiny liquid droplets. Therefore,

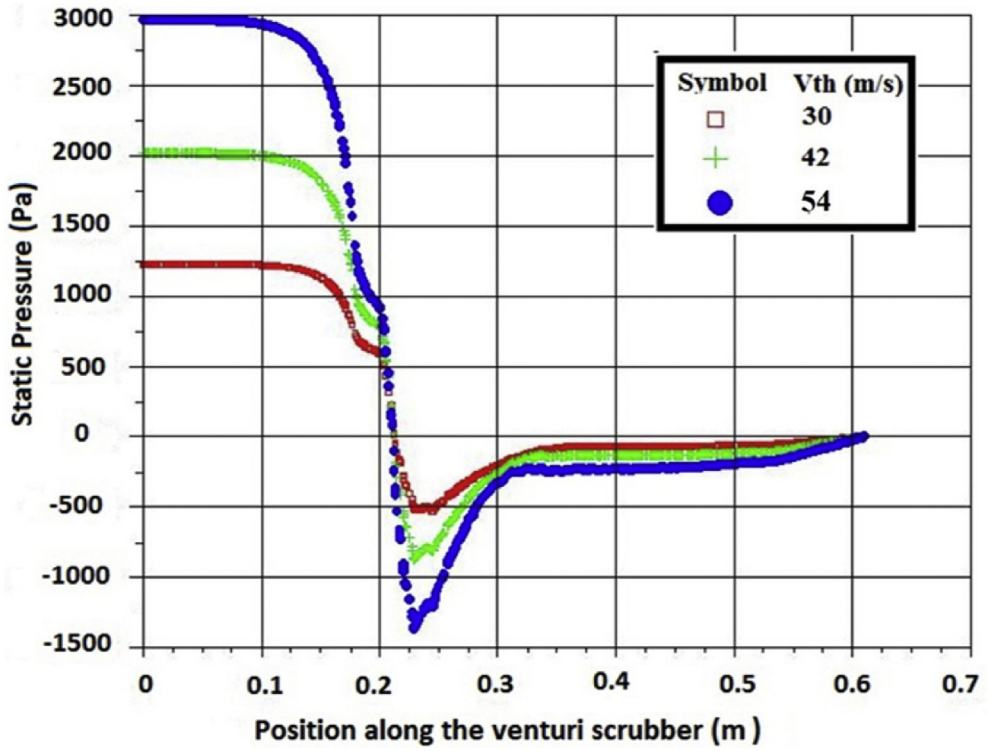

Fig. 2 – Static pressure profile along the Venturi scrubber at different throat gas velocities with constant mass flow rate 0.033 kg/s.

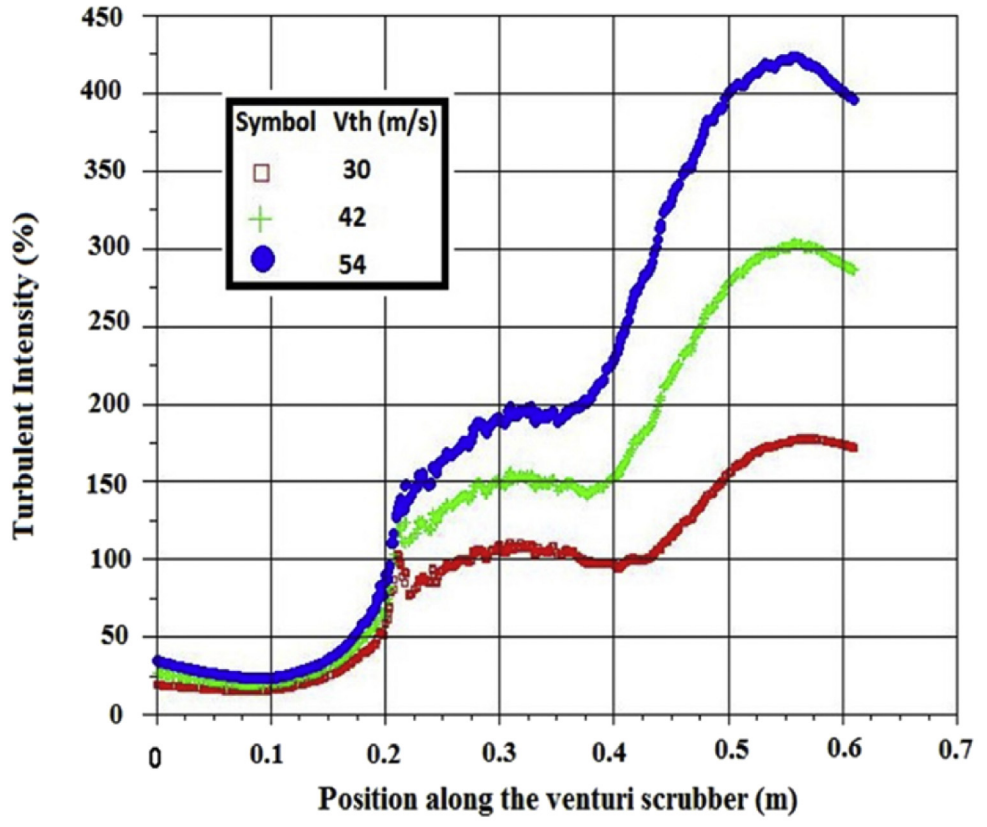

Fig. 3 – Turbulent intensity profile along the Venturi scrubber at different throat gas velocities with constant mass flow rate 0.033 kg/s.

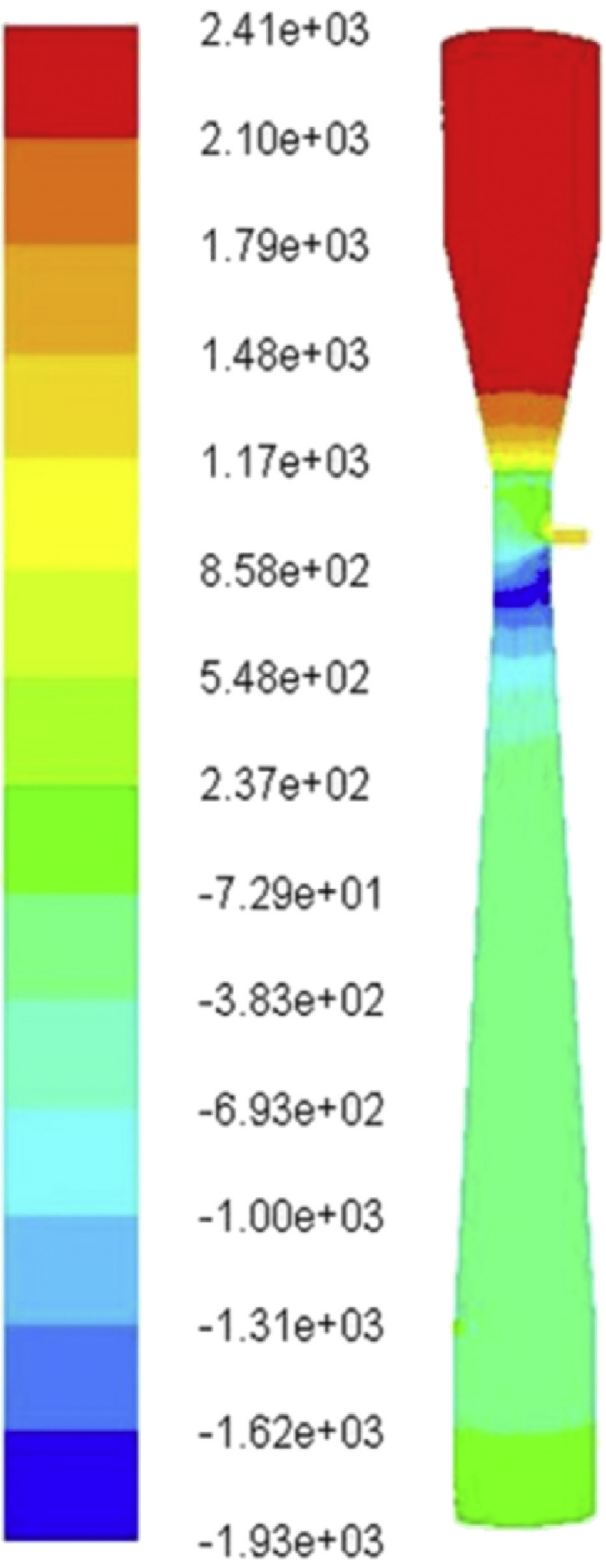

Fig. 4 – Contour of static pressure at liquid mass flow rate 0.016 kg/s and throat gas velocity 60 m/s.

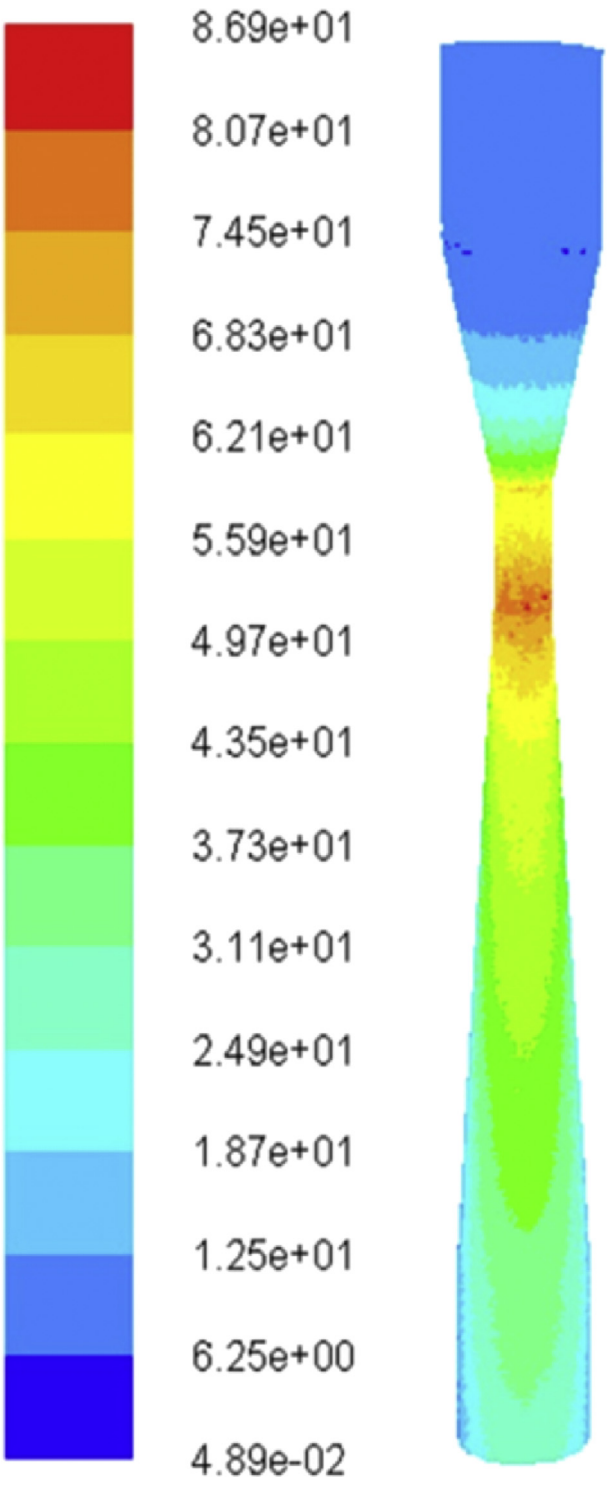

Fig. 5 – Contour of velocity magnitude at liquid mass flow rate 0.016 kg/s and throat gas velocity 60 m/s.

particles are captured by the liquid droplets by inertial impaction. Removal efficiency of particle depends on the pressure drop of the venturi scrubber system. Therefore, it is important to study the hydrodynamics of venturi scrubber. Operating parameters those are effecting the pressure drop are throat gas velocity, liquid flow rate, liquid loading and gas mass flow rate. Present research is conducted at different throat gas velocity and liquid flow rate. Distribution of pressure, velocity and turbulence are also observed. The venturi scrubber is simulated by varying throat gas velocity from 24 m/s to 60 m/s and mass flow rate from 0.016 kg/s to 0.033 kg/s for liquid is used.

Fig. 2 indicates the gas acceleration occurs in the convergent section due to transformation of pressure into kinetic energy. Gas reaches the maximum velocity at the throat section; therefore, pressure continues to drop because of the friction of maximum velocity with the wall. In the diffuser, gas recovers some pressure due to loss in velocity. All the kinetic energy obtained in the form of pressure at entry of the throat is not return to the diffuser because of turbulent and viscous

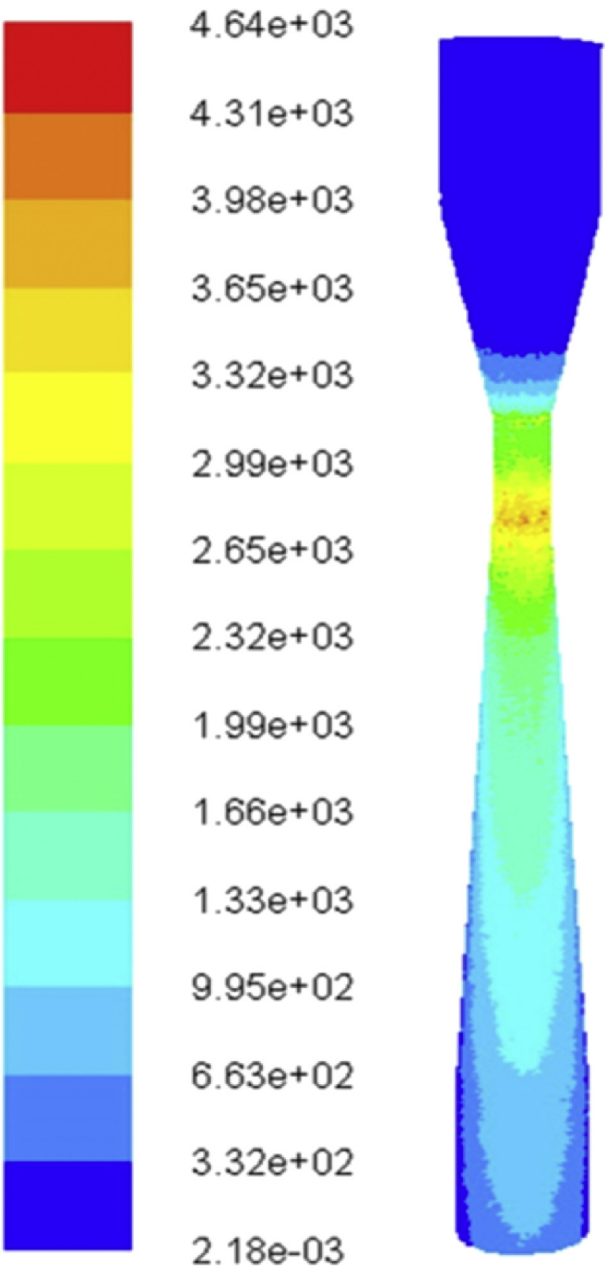

Fig. 6 – Contour of dynamic pressure at liquid mass flow rate 0.016 kg/s and throat gas velocity 60 m/s.

dissipations. So, static pressure at the entrance is higher than the exit. In the Fig. 3, it is observed that turbulent intensity increases in the diffuser section. This is because of the more velocity fluctuation occurring in that zone due to extending the region to the channel exit.

The contours of static pressure, velocity magnitude and dynamic pressure displayed in Figs. 4–6. Figs. 4 and 5 shows the static pressure fields and velocity field respectively in the venturi scrubber. From the figures, it can be seen maximum pressure drop and maximum gas velocity are observed in the throat section due to small section causes friction with maximum gas velocity and wall. Beyond this point in the diffuser section, pressure drop decreases as well as velocity decreases due to divergence of the channel. Fig. 6 indicates the dynamic pressure field. The dynamic pressure is basically proportional to the square of the velocity. From the Fig. 6, it can be observed that the dynamic pressure and the velocity have approximately the same profile in the scrubber. The dynamic pressure increases from the inlet to the throat and decreases from the throat to the outlet. The highest values are observed in the venturi throat due to higher velocity. Fig. 7 indicates the velocity vector distribution inside the venture scrubber.

5.1. *Effect of throat gas velocity on pressure drop*

Fig. 8 shows the dependence of the throat gas velocity on the pressure drop inside the venturi scrubber. From the figure, it may be seen that the pressure drop increases with throat gas velocity. This was mainly occurred due to the friction of maximum gas velocity with the wall. When gas passes through the small concentric throat section resulting the maximum gas velocity which causes the large friction within this region, so high pressure drop generates. If throat gas velocity increases, large amount of friction can be generated, achieved the higher pressure drop. This behaviour agrees with the results shown in the literature (Leith and Cooper, 1980; Gonçalves et al., 2001; Guerra et al., 2009). Maximum pressure drop occur with the highest throat gas velocity 60 m/s.

5.2. *Effect of liquid mass flow rate on pressure drop*

Effect of liquid mass flow rate on pressure drop at various throat gas velocity is presented in Fig. 9. It shows that the pressure drop increases with increasing liquid mass flow rate. This is quite obvious as, with increase in liquid mass flow rate, the inertia encountered by the gas in the scrubber in presence of liquid droplets is more. It is interesting to note that with increase in liquid mass flow rate and throat gas velocity, the deviation is more at higher liquid mass flow rate than at lower liquid mass flow rate. This may be due to the fact that, the pressure energy lost at larger throat gas velocity to overcome the resistances offered by high gas velocity and large number of droplets is significant. As a result the deviation is more at higher liquid flow rates. Maximum pressure drop obtained at the highest liquid flow rate 0.033 kg/s.

5.3. *Effect of liquid/gas ratio on pressure drop*

Fig. 10 indicates the dependence of liquid/gas ratio on pressure drop. Pressure drop increases with liquid/gas loading at constant throat gas velocity. Stronger influence of L/G ratio indicates a greater degree of energy transfer from the gas to liquid phase.

5.4. *Effect of gas flow rate on pressure drop*

From the Fig. 11, it is clearly observed that the increase in gas flow rate, pressure drop increases. If gas mass flow rate increases, throat gas velocity also increases. So, higher throat gas velocity causes the higher friction and higher momentum transformation between gas and liquid droplets.

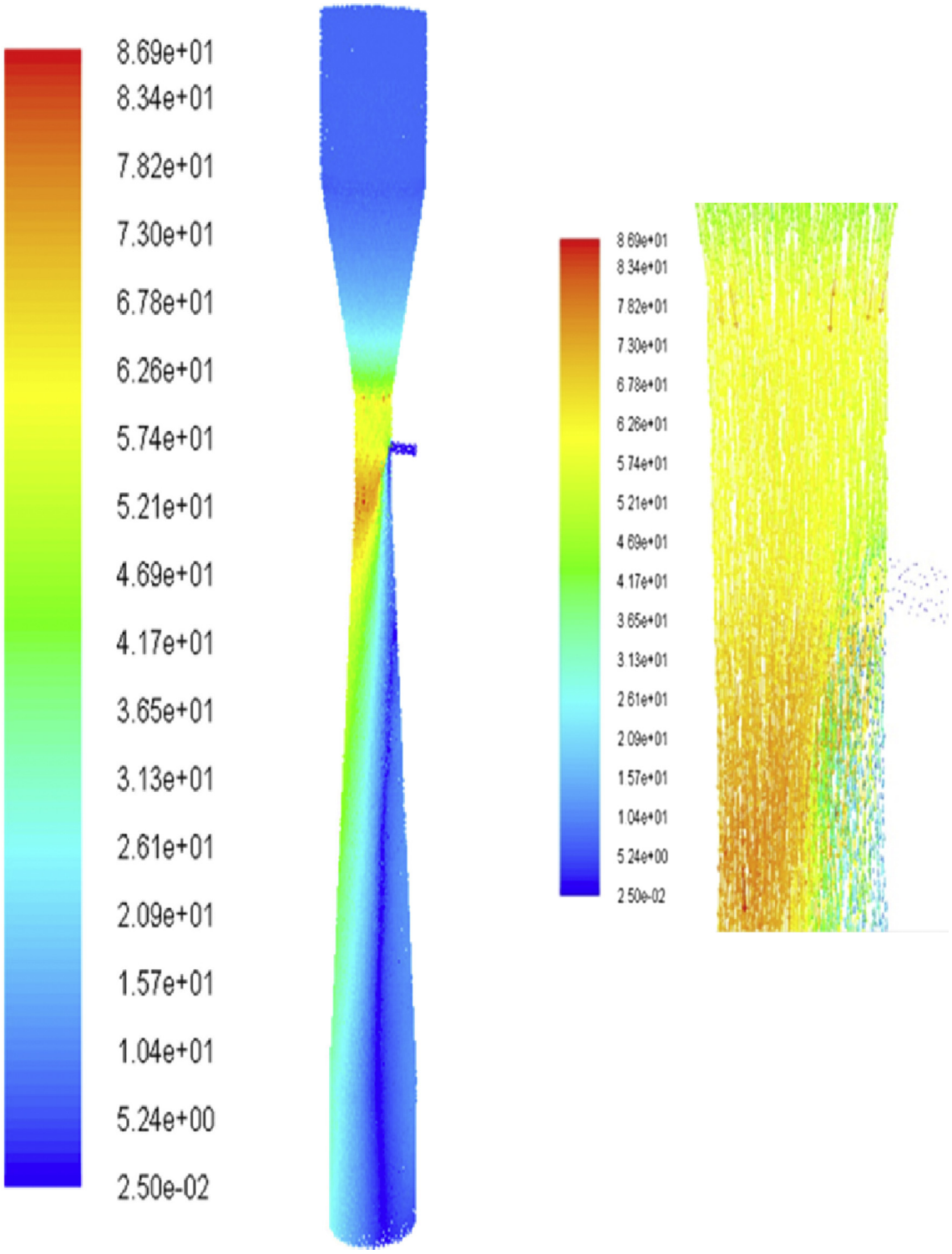

Fig. 7 – Contour of velocity vector (m/s) at liquid mass flow rate 0.016 kg/s and throat gas velocity 60 m/s.

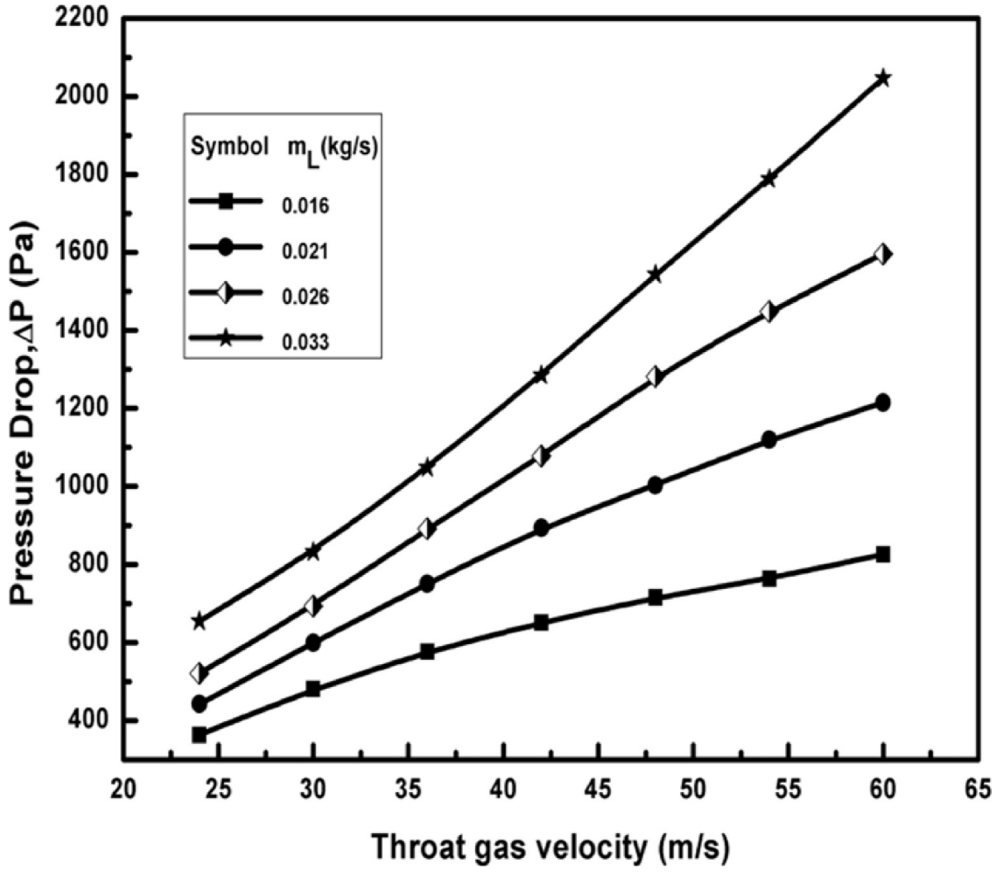

Fig. 8 – The effect of throat gas velocity on the pressure drop.

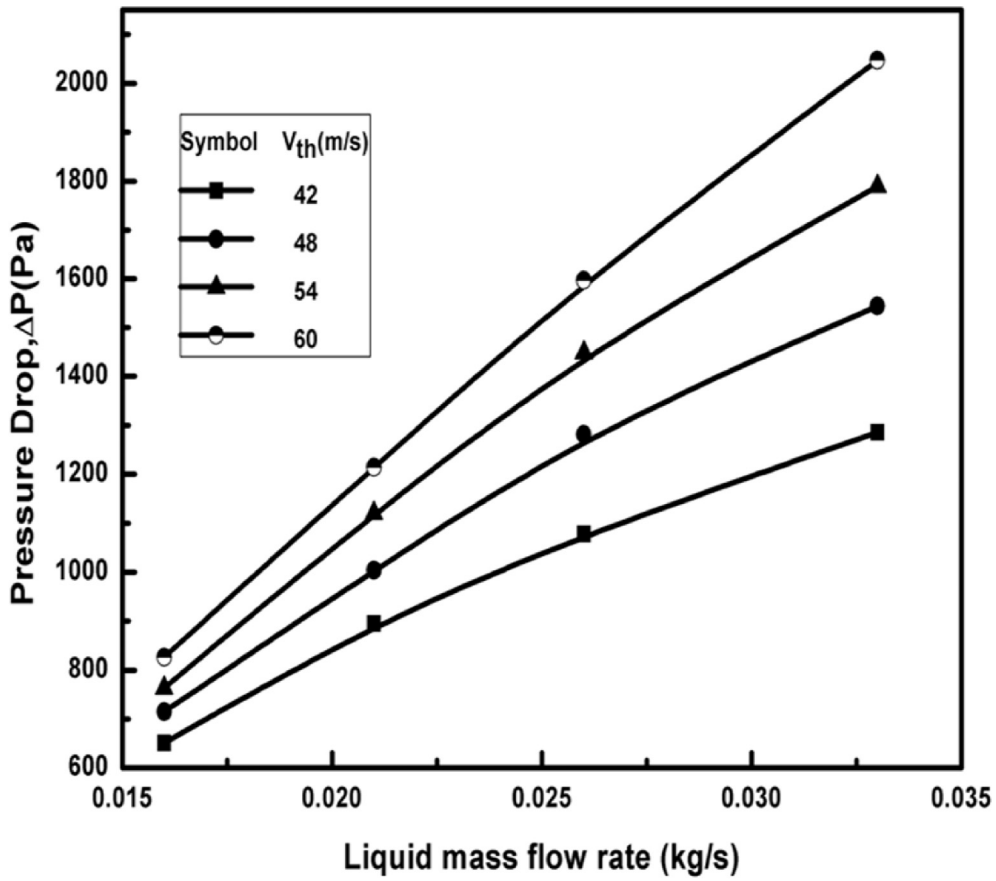

Fig. 9 – The effect of liquid mass flow rate on the pressure drop.

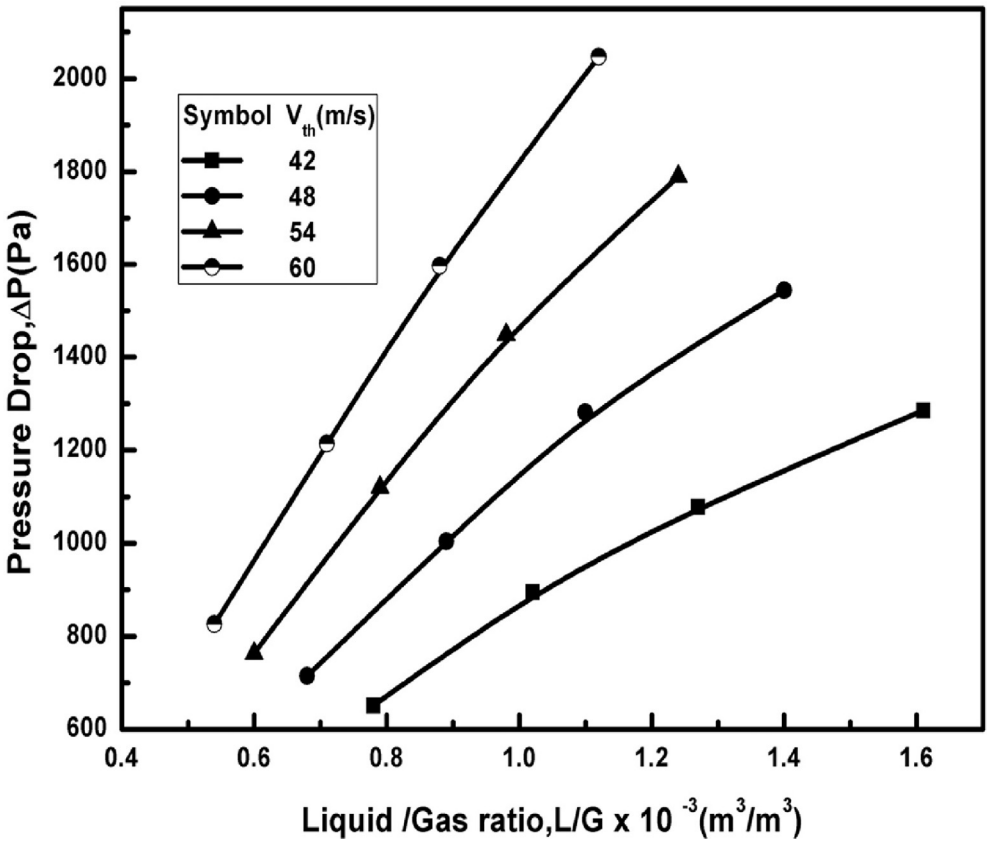

Fig. 10 – The effect of the L/G ratio on the pressure drop.

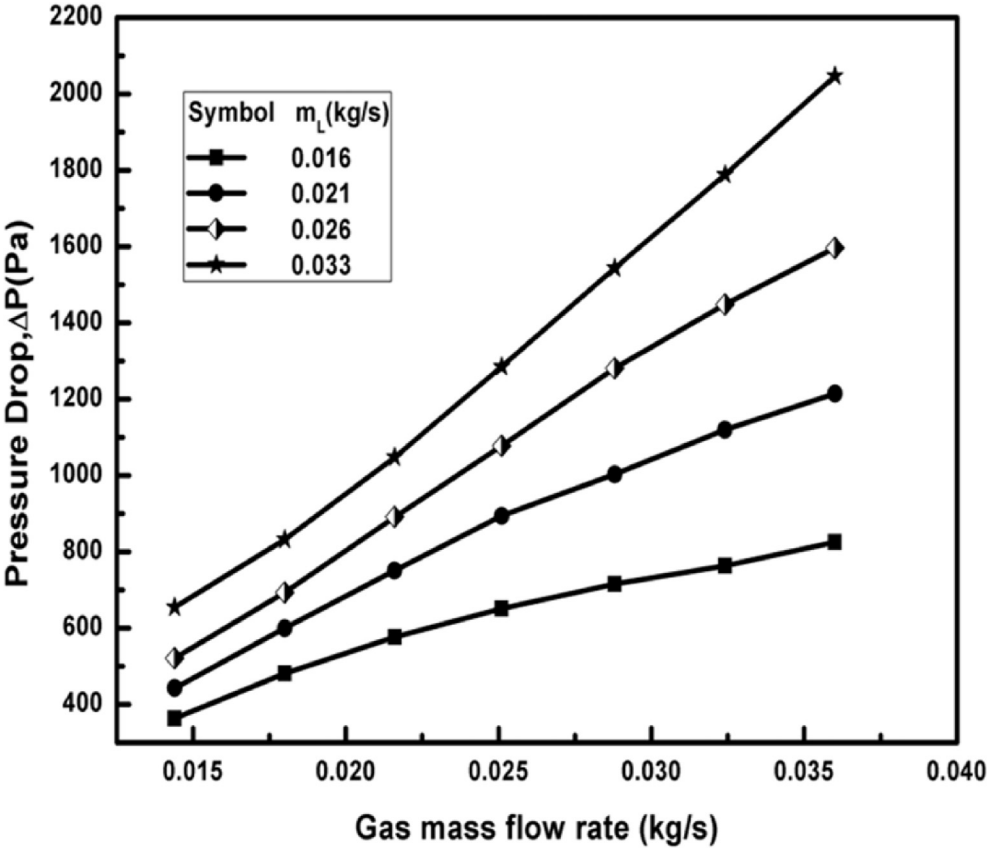

Fig. 11 – The effect of gas mass flow rate on the pressure drop.

6. Conclusion

A venturi scrubber was fabricated and designed to be used as an air pollution control device. Gas enters through the convergent section and maximized the velocity at the throat section. Scrubbing liquid water was injected at the throat section and produce small droplets by contacting with the maximized gas velocity. A numerical model had been adopted to determine the hydrodynamic property in terms of pressure drop inside the venturi scrubber. Fluent software had been used to study the hydrodynamics. Three hydrodynamic parameters like throat gas velocity, liquid mass flow rate and liquid to gas ratio were varying to study hydrodynamic property. The pressure drop was found to increase with throat gas velocity, liquid mass flow rate, and liquid to gas ratio. The maximum pressure drop was found to be 2064.34 pa at the throat gas velocity of 60 m/s and liquid flow rate of 0.033 kg/s and minimum pressure drop 373.51 pa was achieved at the throat gas velocity of 24 m/s and liquid flow rate of 0.016 kg/s. The hydrodynamic result for higher pressure drop signifies higher collection efficiency but this leads to higher pumping cost. Hydrodynamics study has been carried out to design the venturi scrubber and to determine the optimal pressure drop for the removal of iodine.

Appendix A. Supplementary data

Supplementary data related to this article can be found at https://doi.org/10.1016/j.sajce.2017.10.006.

References

ANSYS Inc, 2015. ANSYS Fluent Meshing User's Guide.

ANSYS Inc, 2015. ANSYS: Fluent User's Guide.

Ahmadvand, F., Talaie, M.R., 2010. CFD modeling of droplet dispersion in a Venturi scrubber. Chem. Eng. J. 160, 423–431.

Ali, M., Chang, Y., Zhong, S., Jianand, W., Mehboob, K., 2012. CFD Simulation of Prediction of Pressure drop in venturi scrubber. Appl. Mech. Mater. 166–169, 3008–3011.

Ali, M., Changqi, Y., Zhongning, S., Jianjun, W., Haifeng, G., Mehboob, K., 2013. Dust particle removal efficiency of a venturi scrubber. Ann. Nucl. Energy 54, 178–183.

Ananthanarayanan, N.V., Viswanathan, S., 1999. Effect of nozzle arrangement on venturi scrubber performance. Ind. Eng. Chem. Res. 38, 4889–4900.

Bayatian, M., Ashouri, M.R., Mahmoudkhani, R., 2016. Flow behavior simulation with computational fluid dynamics in spray tower scrubber. Int. J. Environ. Sci. Dev. 7 (3), 181–184.

Biswas, S., Rajmohan, B., Meikap, B.C., 2008. Hydrodynamics of counter-current spray column. Asia Pac. J. Chem Eng 3, 544–549.

Boll, R.H., 1973. Particle collection and pressure drop in venturi scrubber. Ind. Eng. Chem. Fundam. 12 (1), 40–49.

Calvert, S., 1970. Venturi and other Atomizing Scrubbers efficiency and pressure drop. AICHE J. 16 (3), 392–396.

Desai, R., Sahu, O.P., 2014. Study of venturi scrubber efficiency for pesticide industry. Int. Lett. Nat. Sci. 4, 15–26.

Fathikalajahi, J., Talaie, M.R., 1997. The effect of droplet size distribution on liquid dispersion in a venturi scrubber. J. Aerosol Sci. 28 (Suppl. 1), S291–S292.

Gamisans, X., Sarr, M., Lafuente, F.J., Azzopardi, B.J., 2002. The hydrodynamics of ejector venturi scrubbers and their modelling by an annular flow/boundary layer model. Chem. Eng. Sci. 57, 2707–2718.

Goniva, C., Tukovic, Z., Feilmayr, C., Burgler, T., Pirker, S., 2009. Simulation of offgas scrubbing by a combined Eulerian–Lagrangian model. In: Seventh International Conference on CFD in the Minerals and Process Industries. CSIRO, Melbourne, Australia.

Gonçalves, J.A.S., Fernández Alonso, D., Martins Costa, M.A., Azzopardi, B.J., Coury, J.R., 2001. Evaluation of the models available for the prediction of pressure drop in Venturi scrubbers. J. Hazard. Mater. B81, 123–140.

Guerra, V.G., Bettega, R., Goncalves, J.A.S., Coury, J.R., 2009. Experimental investigation on the effect of liquid injection by multiple orifices in the formation of droplets in a Venturi scrubber. J. Hazard. Mater. 161, 351–359.

Guerra, V.G., Bettega, R., Goncalves, J.A.S., Coury, J.R., 2012. Pressure drop and liquid distribution in a venturi scrubber: experimental data and CFD simulation. Ind. Eng. Chem. Res. 51, 8049–8060.

Gulhane, N.P., Kadam, H.S., Kale, S.S., 2015. Analysis of pressure and velocity at the throat of self –priming venturi scrubber. J. Mater. Sci. Mech. Eng. 2 (6), 57–61.

Leith, D., Cooper, D.W., 1980. Venturi scrubber optimization. Atmos. Environ. 14, 657–664.

Leith, D., Cooper, D.W., Rudnick, S.N., 1985. Venturi scrubbers: pressure loss and regain. Aerosol. Sci. Technol. 4, 239–243.

Pak, S.I., Chang, K.S., 2006. Performance estimation of a venturi scrubber using a computational model for capturing dust particles with liquid spray. J. Hazard. Mater. 138, 560–573.

Rust, H., Tännler, Ch, Heintz, W., Haschke, D., Nuala, M., Jakab, R., 1995. Pressure release of containments during severe accidents in Switzerland. Nucl. Eng. Des. 157, 337–352.

Shozugawa, K., Nogawa, N., Matsuo, M., 2012. Deposition of fission and activation products after the Fukushima Daiichi nuclear power plant accident. Environ. Pollut. 163, 243–247.

Sripriya, R., Kaulaskar, M.D., Chakraborty, S., Meikap, B.C., 2007. Studies on the performance of a hydrocyclone and modelling for flow characterization in presence and absence of air core. Chem. Eng. Sci. 62, 6391–6402.

Swamy, K., Kumar, N., Meikap, B.C., 2015. Hydrodynamic study of multi-stage plate column scrubber for removal of particulate. S. Afr. J. Chem. Eng 20, 44–60.